Functional imaging of malignant paragangliomas and carcinoid tumours

C. Le Rest, J.B. Bomanji, D.C. Costa, C.E. Townsend, D. Visvikis, P.J. Ell

Institute of Nuclear Medicine, Middlesex Hospital, Mortimer Street, London W1N 8AA, UK

Received 28 October and in revised form 28 December 2000 / Published online: 17 February 2001

Abstract. Complete staging is mandatory for the management and therapy of neuroendocrine tumours. Various radiotracers are available but the best imaging strategy has yet to be defined. In this study we retrospectively compared ^{123}I-MIBG, ^{111}In-[D-Phe^{1}]-DTPA-octreotide and ^{18}F-FDG (PET) imaging in 15 patients with metastatic neuroendocrine tumours (11 carcinoid tumours, 4 paragangliomas). Planar images were acquired 1, 4, 24 and 48 h following the injection of ^{111}In-[D-Phe^{1}]-DTPA-octreotide and ^{123}I-MIBG. Whole-body PET scans were performed 45 min after injection of ^{18}F-FDG. ^{111}In-[D-Phe^{1}]-DTPA-octreotide was positive in 11/15 patients and identified 44 lesions, ^{18}F-FDG PET was positive in 11/15 patients and identified 107 lesions and ^{123}I-MIBG was positive in 8/15 patients and identified 67 lesions. No single scintigraphic technique identified all metastatic sites. In one patient all studies were negative. ^{18}F-FDG PET identified more abnormal sites than the other two modalities. Combination of all three imaging modalities with X-ray CT helps to provide a more comprehensive map of the disease.

Keywords: Neuroendocrine tumours – Carcinoid – Paraganglioma – Metastases – Imaging

Eur J Nucl Med (2001) 28:478–482
DOI 10.1007/s002590100475

Introdcution

Neuroendocrine tumours are derived from the diffuse neuroendocrine system, which is made up of peptide- and amine-producing cells with different hormonal and metabolic profiles depending on their site of origin [1]. The term "neuroendocrine tumour" has been applied specifically to those tumour cells that are characterised by the presence of secretory granules, which represent storage vesicles of either hormones or peptides. Phaeochromocytomas, paragangliomas, carcinoid tumours, medullary carcinomas of thyroid and pancreatic endocrine tumours [1, 2], fall into this category. In this study we addressed the issue of imaging malignant paragangliomas and carcinoid tumours.

The presentation of these tumours is diverse, being related to autonomous hypersecretion of characteristic hormones from their tissue of origin and non-specific neoplastic behaviour such as local invasion and distant spread of disease. Paragangliomas are uncommon neoplasms, and malignancy is rare and typically defined by the existence of metastases rather than by cellular characteristics. Treatment usually revolves around debulking or radiation therapy and ^{131}I-metaiodobenzylguanidine (^{131}I-MIBG) therapy [3]. In the case of carcinoid tumours, it is difficult to differentiate benign from malignant carcinoid based on histology. Malignancy can only be unequivocally determined if there is lymph node invasion or distant metastases [4]. Thus in both conditions, detection of the full extent of distant spread is important for management and prognosis.

In this retrospective analysis, we report our original findings and share our experience of using ^{123}I-MIBG, ^{111}In-[D-Phe^{1}]-DTPA-octreotide and ^{18}F-fluorodeoxyglucose (^{18}F-FDG) imaging in patients with malignant paragangliomas and carcinoid tumours.

Materials and methods

Patient population. We reviewed the data of all patients with neuroendocrine tumours who had undergone imaging at the Institute of Nuclear Medicine, Middlesex Hospital, over the past 2 years. Of the 38 patients reviewed, 15 had undergone imaging with ^{123}I-MIBG, ^{111}In-[D-Phe^{1}]-DTPA-octreotide and ^{18}F-FDG coupled with X-ray computed tomography (CT). All imaging studies were performed within a time span of 40 days.

Of the 15 patients (eight men, seven women; age range 30–71 years, median 54 years), 11 had metastatic carcinoid and four had

J.B. Bomanji (✉)
Institute of Nuclear Medicine, Middlesex Hospital,
Mortimer Street, London W1N 8AA, UK
e-mail: j.bomanji@nucmed.ucl.ac.uk
Tel.: +44-207-3809425, Fax: +44-207-6370578

metastatic paraganglioma. The histological diagnosis was available in all patients.

Of the 11 patients with metastatic carcinoid, five had carcinoid syndrome. In nine patients, the primary site was the bowel (appendix in six, ileum in three), while in two the primary site was unknown. Of the 11 patients, five were being assessed for clinical suspicion of recurrence after previous treatment and three were being reassessed after completing ^{131}I-MIBG therapy. Three patients had been referred for staging as a prelude to ^{131}I-MIBG therapy.

Of the four patients with metastatic paraganglioma, two were non-secretors who had previously been treated with surgery, chemotherapy and radiotherapy and were being reassessed for ^{131}I-MIBG therapy. The other two patients were being evaluated after completing ^{131}I-MIBG therapy.

Imaging procedures. All radionuclide studies were acquired >12 weeks after completion of chemotherapy or ^{131}I-MIBG therapy.

Before scintigraphy with ^{123}I-MIBG, 60 mg b.d. of potassium iodide was administered orally to block the thyroid uptake of any free radioiodine. A mean activity of 200 MBq of ^{123}I-MIBG was slowly injected intravenously. Using a gamma camera, whole-body anterior and posterior views were obtained at 1, 4, 24 and 48 h post injection (scan speed 20 min/m and at 48 h 30 min/m).

^{111}In-[D-Phe^{1}]-DTPA-octreotide (mean activity 150 MBq) was injected intravenously. Whole-body anterior and posterior views were obtained at 4, 24 and 48 h post injection (scan speed 20 min/m and at 48 h 30 min/m).

For ^{18}F-FDG positron emission tomography (PET), patients fasted overnight. Blood glucose levels were checked prior to injection. Each patient received 5 mg of diazepam orally 30 min before the ^{18}F-FDG injection. The whole-body PET scan was acquired 45 min after intravenous injection of ^{18}F-FDG (mean activity 350 MBq). A dedicated state-of-the-art PET scanner (GE Advance) was used for imaging. Emission data were acquired in six 5-min bed positions followed by a whole-body transmission scan using three ^{68}Ge rotating sources (3-min images per bed position). Attenuation-corrected emission data were reconstructed iteratively using an ordered subset expectation maximisation (OSEM) algorithm. ^{18}F-FDG scans were visually reported without the support of standardised uptake values.

Image interpretation. A study was classified as positive if an abnormal site of tracer uptake was identified which corresponded to a known disease site on CT. If no uptake was identified at a suspected site or elsewhere in the body, then the study was classified as negative.

Tracer uptake at tumour sites was assessed for each radiopharmaceutical and compared with the activity of the assumed normal liver. It was classified as "faint" when less intense than liver uptake, and as "high" when equal to or more intense than liver uptake. In the case of liver metastases, uptake was classified as high if it exceeded uptake in the adjacent, assumed normal liver tissue.

The total number of lesions detected by each modality was counted. When an organ was heavily infiltrated, e.g. liver (Fig. 1), a lesion count of one was allocated to that site. In patients in whom a large tumour mass (>2×2 cm) was identified, a comparison of tracer distribution pattern in the mass was carried out for all three modalities.

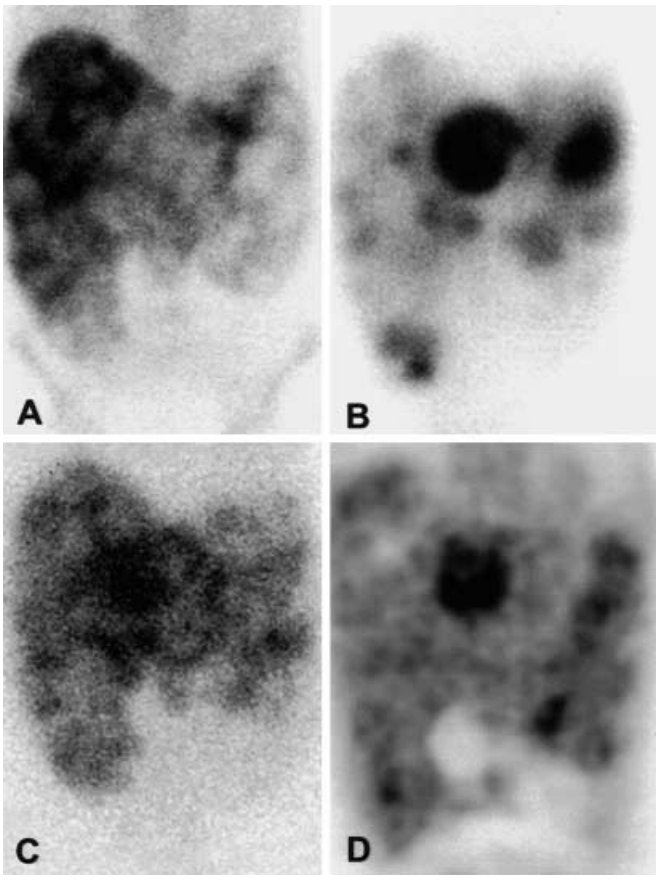

Fig. 1A–D. Patient with extensive liver metastases from carcinoid tumour. **A** ^{99m}Tc-colloid scan shows multiple "cold" areas. **B** ^{111}In-[D-Phe^{1}]-DTPA-octreotide scan shows multiple metastases. Two large areas with "high" uptake and homogeneous distribution of tracer are seen. A smaller area with non-homogeneous distribution is noted in the tip of the right hepatic lobe. These avid lesions correspond to the "cold" areas noted on the colloid scan. **C** ^{123}I-MIBG scan shows multiple metastases, but a pattern which is different from the ^{111}In-[D-Phe^{1}]-DTPA-octreotide distribution (one of the two large areas with "high" uptake is not visualised). **D** ^{18}F-FDG PET scan (coronal section) shows the two large liver metastases to be glucose avid, but a different distribution pattern elsewhere (range of SUVgl, 10–30)

Results

In 12 of the 15 patients no more than two of the three radionuclide imaging modalities were positive. In two patients with carcinoid disease all three radionuclide studies were positive, while in one patient, also with carcinoid disease, all radionuclide imaging studies were negative. The most common metastatic site was the liver (Table 1).

Both ^{111}In-[D-Phe^{1}]-DTPA-octreotide receptor scintigraphy and ^{18}F-FDG PET demonstrated abnormally increased tracer uptake in 11 of the 15 patients, while ^{123}I-MIBG did so in eight (Table 2). The intensity of tracer uptake at tumour sites was "high" in 93% with ^{18}F-FDG

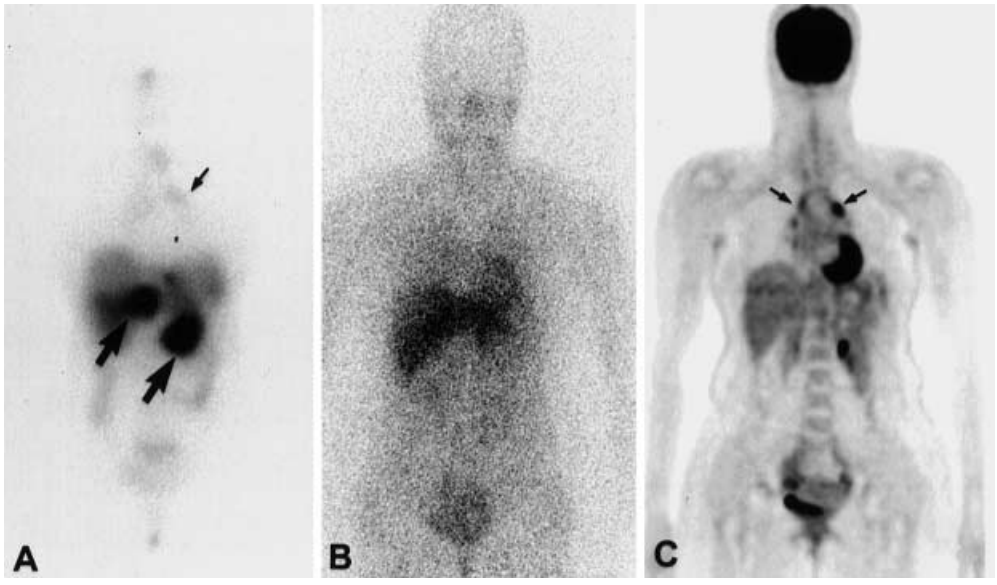

Fig. 2A–C. Patient with carcinoid metastases to liver and mesentery coupled with hilar activity. **A** ^{111}In-[D-Phe^{1}]-DTPA-octreotide scan shows two large metastases with "high" uptake (*large arrows*), one in the liver and one in the mesentery. In addition, there is a small liver metastasis in the left hepatic lobe. Note the "faint" hilar activity (*small arrow*). **B** A negative ^{123}I-MIBG scan. **C** ^{18}F-FDG PET scan shows "high" uptake in hilar nodes and the mesenteric metastases. The liver metastases showed "faint" uptake (anterior section not shown)

Table 1. Sites of metastases in patients with carcinoid tumours or paragangliomas

Sites involved	Metastatic carcinoid (*n*=11)	Metastatic paraganglioma (*n*=4)
Liver/pancreas	10/11	1/4
Bone/bone marrow	3/11	3/4
Bowel/omentum	2/11	–
Lymph nodes/sympathetic chain	2/11	4/4
Lung fields	2/11	2/4

Table 2. Total number of lesions identified by each of the three imaging modalities in the two groups of patients

	^{111}In-Oct		^{18}F-FDG		^{123}I-MIBG	
	No. of pts +ve	No. of lesions detected	No. of pts +ve	No. of lesions detected	No. of pts +ve	No. of lesions detected
Metastatic carcinoid (11 pts)	10	38	8	36	4	16
Metastatic paraganglioma (4 pts)	1	6	3	71	4	51
Total	11	44	11	107	8	67

PET, 85% with ^{111}In-[D-Phe^{1}]-DTPA-octreotide and 62% with ^{123}I-MIBG.

In patients in whom two of the three imaging studies were positive, more than two lesions were positive with one modality and negative with the other. ^{18}F-FDG PET identified 107 lesions, ^{111}In-[D-Phe^{1}]-DTPA-octreotide 44 lesions and ^{123}I-MIBG 67 lesions (Table 2). Three patients with carcinoid had extensive liver metastases and two with metastatic paraganglioma showed widespread bone/bone marrow involvement.

In six patients a single large (>2×2 cm) tumour site was identified. In four, tracer uptake was fairly homogeneous in distribution and the intensity of uptake was "high" for all three tracers. In the other two cases, tracer distribution was non-homogeneous, with a different distribution pattern and variable intensity of uptake for all three tracers.

One patient with carcinoid tumour was negative on all imaging modalities, including CT. This patient had recently had the tumour resected from the ileum. The operation was felt to be complete, but a mesenteric biopsy showed a small focus of metastatic tumour.

In one carcinoid patient with liver metastases, ^{111}In-[D-Phe^{1}]-DTPA-octreotide scan showed additional "faint" bilateral hilar activity, which the ^{18}F-FDG PET scan revealed to represent focal hilar nodes with "high" avidity for glucose (Fig. 2). ^{123}I-MIBG scan was negative and X-ray CT did not identify any abnormal hilar nodes in this patient.

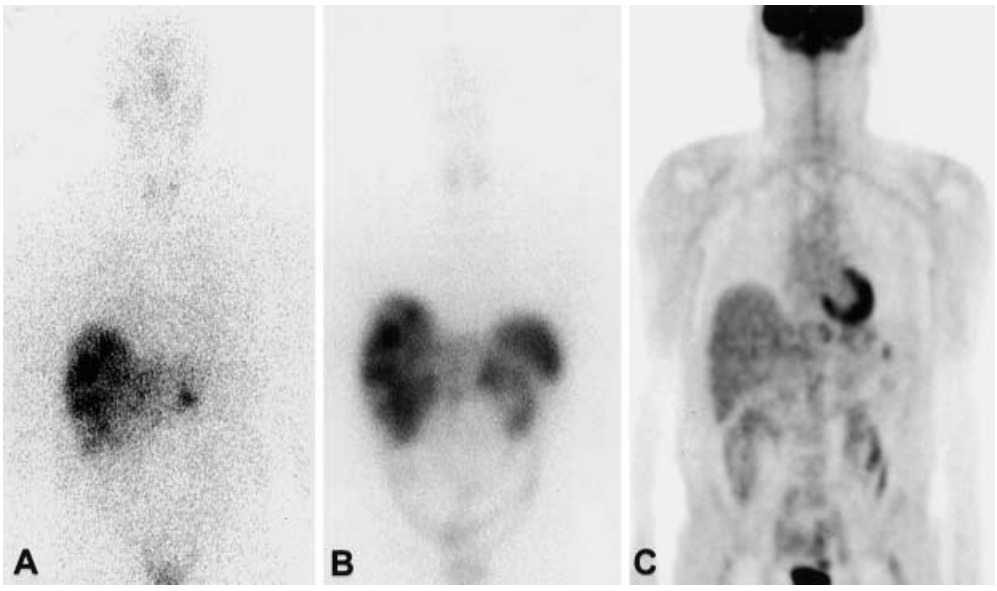

Fig. 3A–C. Patient with carcinoid liver metastases treated with ^{131}I-MIBG (cumulative dose 39.7 GBq). **A** ^{123}I-MIBG scan and **B** ^{111}In-[D-Phe^{1}]-DTPA-octreotide scans show "high" uptake in liver metastases. **C** ^{18}F-FDG PET scan was negative

Only one patient with metastatic carcinoid disease had positive ^{111}In-[D-Phe^{1}]-DTPA-octreotide scintigraphy and ^{123}I-MIBG scan but a negative ^{18}F-FDG PET study (Fig. 3). This patient had completed a course of ^{131}I-MIBG therapy (cumulative dose 39.7 GBq) 12 weeks prior to the imaging studies. Follow-up CT 6 months following therapy showed no significant change in tumour size.

In 14 patients CT clearly identified metastases to liver, mediastinum and the abdomen which corresponded to the areas of tracer uptake observed on scintigraphy. In addition, scintigraphy identified eight lesions not seen on CT. In two patients the initial CT examination was not extended above the diaphragm, so mediastinal metastases subsequently shown with scintigraphy were not identified.

Discussion

This study clearly shows that none of the imaging modalities, alone or in combination, provides a comprehensive survey of disease spread in patients with paragangliomas and carcinoid tumours.

^{18}F-FDG PET detected the most tumour metastases, followed by ^{123}I-MIBG scan (though ^{111}In-[D-Phe^{1}]-DTPA-octreotide identified metastases in 11/15 patients whereas ^{123}I-MIBG scan did so in only 8/15). Each of the modalities was completely negative in at least one patient, while the others were positive. Interestingly, within-lesion distribution of the tracers was also variable, with part of a tumour mass showing affinity for one tracer, and another part showing affinity for another tracer. These imaging features reflect the very diverse nature of these tumours. We have previously shown such variable tracer distribution for ^{123}I-MIBG [5] and ^{111}In-[D-Phe^{1}]-DTPA-octreotide [6, 7], while others have demonstrated a similar pattern using ^{18}F-FDG PET and ^{111}In-[D-Phe^{1}]-DTPA-octreotide [8] and ^{18}F-FDG PET and ^{123}I-MIBG [9]. To our knowledge, however, there has been no direct comparison of all three imaging modalities.

The inability to localise all tumour sites also has implications for therapy with ^{131}I-MIBG, ^{111}In-[D-Phe^{1}]-DTPA-octreotide and ^{90}Y-DOTATOC [10, 11, 12]. Individually, or in combination, these radiopharmaceuticals will not achieve total tumour kill. Thus only a partial tumour response may be achieved. This partly explains and reinforces our and other groups' experience in achieving a partial therapeutic response in treating these neoplasms.

In this series, five patients (three with carcinoid, two with paragangliomas) were reviewed 12 weeks after completion of ^{131}I-MIBG therapy (cumulative dose of 33–39.7 GBq). Residual disease was identified in all patients with ^{123}I-MIBG. ^{18}F-FDG PET was positive in three and negative in two of the patients (both patients in whom ^{18}F-FDG PET was negative had carcinoid). The complete lack of uptake observed on ^{18}F-FDG PET in the latter patients was difficult to explain (Fig. 3), though it can be speculated that the tumour had switched to a less aggressive mode or that this picture represents a form of tumoural hibernation.

Scintigraphy revealed some interesting features which merit attention. ^{111}In-[D-Phe^{1}]-DTPA-octreotide and ^{18}F-FDG PET revealed hilar activity in a carcinoid patient with metastatic liver disease (Fig. 2). The aetiology of this activity was difficult to explain as CT of this site failed to reveal any nodal involvement. The liver metastases were subsequently resected; however, no intervention was carried out to confirm the nature of the hilar activity. It is known that both ^{111}In-[D-Phe^{1}]-DTPA-octreotide and ^{18}F-FDG PET can identify granulomatous conditions [13, 14], but there was no clinical, radiological or

biochemical evidence to support this impression. A follow-up ^{111}In-[D-Phe^{1}]-DTPA-octreotide study performed 6 months later showed persistent nodal activity which, compared with the previous study, was extremely faint. It could be argued that this activity represented metastases, but the observed reduction in activity stands contrary to such a conclusion.

A second interesting case was the carcinoid patient who was negative on all imaging modalities, including CT. It was clear that the patient had low-bulk or minimal residual disease, but there was biopsy-proven evidence that metastasis to the mesentery had occurred. A recent CT (15 months after surgery) was unremarkable, and the patient's clinical status remains unchanged. It can only be speculated that the mesenteric seedlings could not be visualised because tracer uptake was faint and was being masked by overlying non-specific gut activity, which is usually seen with all three scintigraphic techniques.

Some of the limitations of this study need to be discussed. This retrospective analysis was triggered on the basis of observation of scintigraphic variation in two patients with neuroendocrine tumours. Prior to embarking on a prospective controlled study, a retrospective analysis of existing data was necessary to understand the observed scintigraphic discrepancies. Our data trawl yielded a very heterogeneous mix of patients at different stages of disease. This was not surprising, as selecting a large number of cases at a specific stage in rare conditions such as carcinoid and paraganglioma is fraught with difficulties. This problem was further compounded by the stipulation that patients must have undergone ^{123}I-MIBG, ^{111}In-[D-Phe^{1}]-DTPA-octreotide and ^{18}F-FDG PET imaging coupled with CT within a short interval. Thus only a relatively small number of patients could be included for observational analysis and no statistical evaluation was undertaken. No attempts were made to compare scintigraphic lesion count with CT as this was not the purpose of our review. Previous comparisons of CT with ^{123}I-MIBG have shown the advantages and limitations of scintigraphic and CT techniques [15], and these continue to hold true.

Conclusion

- This retrospective observational study of patients with metastatic paragangliomas and carcinoid tumours clearly illustrates the variation in tumour affinity for ^{123}I-MIBG, ^{111}In-[D-Phe^{1}]-DTPA-octreotide and ^{18}F-FDG.
- No single scintigraphic technique identifies all the metastatic sites in this group of patients.
- The metastases show either “faint” or “high” uptake of tracer.

While they tend to display notable affinity for ^{18}F-FDG, it is concluded that any single tumour mass may show similar or variable affinity for the three radiopharmaceuticals.

References

1. Kloppel G, Heitz PU. Classification of normal and neoplastic neuroendocrine cells. *Ann NY Acad Sci* 1994; 733:19–23.
2. Langley K. The neuroendocrine concept today. *Ann NY Acad Sci* 1994; 733:1–17.
3. Sessions RB, Harrison LB, Forastiere AA. Tumours of the salivary glands and paragangliomas. In: DeVita VT, Hellman S, Rosenberg S, eds. *Cancer: principles and practice of oncology, 5th edn.* Philadelphia: Lippincott-Raven; 1997:830–847.
4. Jensen RT, Norton JA. Carcinoid tumours and the carcinoid syndrome. In: DeVita VT, Hellman S, Rosenberg S, eds. *Cancer: principles and practice of oncology, 5th edn.* Philadelphia: Lippincott-Raven; 1997:1704–1723.
5. Bomanji J, Levison DA, Zuzarte J, Britton KE. Imaging of carcinoid tumours with I-123-meta–iodobenzylguanidine. *J Nucl Med* 1987; 28:1907–1910.
6. Bomanji J, Mather SJ, Ur E, Moyes J, Grossman A, Britton KE, Besser GM. A scintigraphic comparison of I-123 metaiodobenzylguanidine (MIBG) and an I-123 labelled somatostatin analogue (Tyr-3-octreotide) in metastatic carcinoid tumours. *J Nucl Med* 1992; 33:1121–1124.
7. Hoefnagel C. Metaiodobenzylguanidine and somatostatin in oncology: role in the management of neural crest tumors. *Eur J Nucl Med* 1994; 21:561–581.
8. Pasquali C, Rubello D, Sperti C, Gasparoni P, Liessi G, Chierichetti F, Ferlin G, Pedrazzoli S. Neuroendocrine tumor imaging: can ^{18}F-fluorodeoxyglucose positron emission tomography detect tumors with poor prognosis and aggressive behavior? *World J Surg* 1998; 22:588–592.
9. Shulkin B, Thompson N, Shapiro B, Francis I, Sisson J. Pheochromocytomas: imaging with 2 [fluorine 18]fluoro-2-D-glucose PET. *Radiology* 1999; 212:35–41.
10. Bomanji J, Britton KE, Ur E, Hawkins L, Grossman A, Besser G. Treatment of malignant phaechromocytoma, paraganglioma and carcinoid tumours with ^{131}I-metaiobenzylguanidine. *Nucl Med Commun* 1993; 14:856–861.
11. Caplin ME, Mielcarek JR, Buscombe JR, Jones AL, Croasdale PL, Cooper MS, Burroughs AK, Hilson AJW. Toxicity of high ^{111}In octreotide therapy in patients with disseminated neuroendocrine tumours. *Nucl Med Commun* 2000; 21:97–102.
12. Cremonesi M, Ferrari M, Zoboli S, Chinol M, Stabin MG, Orsi F, Maecke HR, Jermann E, Robertson C, Fiorenza M, Tosi G, Pagnelli G. Biokinetics and dosimetry in patients administered with ^{111}In-DOTA-Tyr3-octreotide: implications for internal radiotherapy with ^{90}Y-DOTATOC. *Eur J Nucl Med* 2000; 26:877–886.
13. Vanhagen PM, Krenning EP, Reubi JC, Kwekkeboom DJ, Bakker WH, Mulder AH, Laissue I, Hoogstede HC, Lamberts SW. Somatostatin analogue scintigraphy in granulomatous disease. *Eur J Nucl Med* 1994; 21:497–502.
14. Gupta N, Gill H, Graeber G, Bishop H, Hurst J, Stephen J. Dynamic positron emission tomography with F-18 fluorodeoxyglucose imaging in differentiation of benign from malignant lung/mediastinal disease. *Chest* 1998; 114:1105–1111.
15. Bomanji J, Conry B, Britton K, Reznek R. Imaging neural crest tumours with ^{123}I metaiodobenzylguanidine and X-ray computed tomography: a comparative study. *Clin Radiol* 1988; 39:502–506.